7 - 12 SEPTEMBER 2014, KRAKÓW
FORUM ACUSTICUM

Compounded plane wave technique applied to imaging attenuation of ultrasound in tissue structures

Ziemowit Klimonda, Jerzy Litniewski, Andrzej Nowicki
Institute of Fundamental Technological Research, Polish Academy of Sciences, Warsaw, Poland.

Summary

The parametric imaging can enhance ultrasonic examinations that are widely used in medical diagnostics. Attenuation of the wave propagating through the soft tissue reflects the state of the tissue, what is clearly demonstrated in literature. The visualization of the spatial distribution of attenuation may support the diagnosis by accurate discrimination of the lesions from normal tissue at the early stage of the disease. This research is focused on the developing of the method of attenuation estimation from ultrasonic backscatter. It would allow to produce the parametric images from the same data as the standard B-mode images. The attenuation estimation method bases on the spectral mean frequency (f_m) downshift of the propagating pulse, that results from the frequency dependence of attenuation. The f_m was determined (using f_m correlation estimator and trend extraction with Single Spectrum Analysis algorithm) from the ultrasonic echoes scattered in the tissue mimicking phantom which contained a cylinder with the attenuation coefficient higher than in the background. The data acquisition were performed using ultrasonic scanner. The earlier research indicated the effectiveness of attenuation estimation method using the synthetic aperture technique to collect the data. The use of the synthetic transmit aperture scheme to acquire the data results in better attenuation imaging comparing to standard beamforming, however it lower the penetration depth. In this research the compounded plane wave transmit-receiving scheme was used, to improve the penetration range. Compensation for the diffraction effects was included in the data processing. The results indicate suitability of this approach for attenuation imaging. We can measure attenuation in the tissue mimicking materials with the spatial resolution of approximately $10mm$ and accuracy of $0.2dB/(MHz \cdot cm)$. In the presentation, the attenuation images of tissue mimicking phantoms and the images of human liver, obtained in vivo, will be presented.

PACS no. 87.63.D-, 87.63.dh

1. Introduction

Soft tissue imaging using ultrasound waves is widely used technique in medical diagnostics. It is noninvasive, secure and relatively cheap method to look inside the human body. The most common technique is to transmit the ultrasound pulses into the body and next receive the echoes backscattered on local differences in acoustic impedance related with tissue structure. The standard ultrasound image shows the amplitude of received echoes scattered in different regions of tissue and characterize the tissue by its echogenicity. This type of images is called B-mode (from 'brightness' modulation) and is probably the most common in medical ultrasound imaging. However, there are more parameters which could characterize the tissue like attenuation, local speed of sound or elasticity. If it is possible to estimate such parameter with a reasonable resolution one can produce so called parametric images, which presents the spatial distribution of a parameter within the tissue. Such image can give unique information about the state of a tissue and is potentially valuable in medical diagnosis. This cause an increasing interests in parametric imaging and its application.

The research presented in this work is focused on the developing of the method of attenuation estimation from ultrasonic backscatter. The attenuation of ultrasound waves is strictly related with internal micro-structure and the way ultrasound wave interact with tissue. Information about attenuation distribution in tissue is valuable for medical diagnosis. In various publications it has been reported that pathological processes can lead to changes in the mean at-

tenuation coefficient. The changes range from several percent for cirrhotic human liver, through dozens percent for fatty human liver [1], or degenerated bovine articular cartilage [2] to over a hundred percent in case of porcine liver HIFU treatment in vivo [3] or two hundred percent for porcine kidney thermal coagulation [4]. It has been shown that the slope of attenuation coefficient, combined with statistical parameters of image texture can be used to diagnose the diffuse liver disease [5]. It has been also reported that the attenuation coefficient differs for cancerous and healthy tissue [6]. Furthermore, the possibility of prediction of the premature delivery in rats and humans through a noninvasive determination of the ultrasonic attenuation have been investigated and reported [7, 8, 9].

2. Methods

The ultrasonic wave propagating through a soft tissue is attenuated due to absorption and scattering. The amplitude A of the plane wave decreases exponentially with the propagation distance, which can be expressed by equation 1

$$A = A_0 \exp\left(\alpha(f) \cdot x\right), \tag{1}$$

where A_0 is an initial amplitude, $\alpha(f)$ is a frequency dependent attenuation and x is a distance passed by the wave within the tissue.

In the soft tissue the attenuation depends on frequency and can be described by the following empirical expression [10]

$$\alpha(f) = \alpha_1 f^n \tag{2}$$

where α_1 denotes the attenuation coefficient and n is a positive exponent. For the soft tissues, n is typically close to 1 which means that the attenuation increases almost linearly with frequency. In this work we assume that for soft tissue $n = 1$. According to equation 2 higher frequency components of a propagating pulse are attenuated more strongly than lower frequency components. Frequency dependent attenuation cause changes in the pulse spectrum and its virtual shift towards lower frequencies is observed. Assuming the transmitted pulses to be Gaussian, its peak frequency f_p can be expressed from equation 3 [11, 12].

$$f_p = f_0 - \alpha_1 \cdot x \cdot \sigma^2 \tag{3}$$

Therefore, the attenuation coefficient can be calculated according to the equation 4.

$$\alpha_1 = -\frac{1}{\sigma^2}\frac{\Delta f_p}{\Delta x} \tag{4}$$

It was assumed that the peak frequency f_p is equal to spectrum mean frequency f_m. Thus, the pulse mean frequency was estimated and used to attenuation estimation by means of equation 4.

In our approach the mean frequency f_m is directly evaluated from the backscattered radio-frequency (RF) signal along the propagation path by means of the correlation estimator [13]. The estimator works on a fragment of the signal located inside of some time window and the resulting estimate value corresponds to center position of the window. While the window moves along the RF line, the f_m line is formed. Each line of radio-frequency (RF) data was processed by the mean frequency estimator. The resulting f_m lines are characterized by high variance, due to stochastic character of ultrasonic backscatter [14]. Therefore, the f_m lines are next processed by Singular Spectrum Analysis (SSA) method [16] to obtain smooth, decreasing trend. The SSA technique decomposes the input data series into the sum of components which can be interpreted as a trend, oscillatory components and noise (non-oscillatory components). The major applications of the SSA technique are smoothing of time series, finding trends, forecasting and detecting structural changes. Moreover the SSA is easy to use as it needs only one parameter – the window length. The f_m lines smoothed by the SSA are next used in calculation of the attenuation along the propagation path according to equation 4. In order to lower the variance of the attenuation images, additional moving average filtration is performed laterally across several lines of the attenuation image.

Our previous research indicates the suitability of the Synthetic Aperture Focusing Technique (SAFT) as a method to collect the input data for attenuation estimation [15]. The images obtaining by SAFT are characterized by good lateral resolution in the whole imaging area, because SAFT allows for dynamic focusing at every image pixel. This makes the neighboring image lines more statistical independent than in Classical Beamforming (CB) technique and consequently lateral moving average filtration is much more effective. This is done without reduction of the frame rate but for the price of additional data processing. In previous experiments the full Synthetic Transmit Aperture (STA) scheme was used, where single element transmits ultrasound pulse and full, 128 elements aperture receives the backscattered echo. Unfortunately, the STA scheme have important drawbacks. First, the use of a single transmit transducer limits the amplitude of the propagating pulse. This decrease the signal-to-noise ratio (SNR) of receiving signals and impose limitation of possible imaging range. Second, the full STA scan require many transmissions, which limits the framerate.

To overcome this limitations the Plane Wave Imaging (PWI) scheme was used [17]. The PWI is realized using the transducer array. The PWI scheme base on transmision of plane, non-focused waves by application linear delays to all elements of transmit aperture.

The synthetized signal value $(RF(p)_{synt})$ in point p was enumerated from the equation 5,

$$RF(p)_{synt} = \sum_i \sum_j \sum_k RF_{i,j,k}(\tau(p)_{i,j,k}) \qquad (5)$$

where i, j and k are indexes of sequential transmission, transmitting transducer and receiving transducer respectively. Hence, the $RF_{i,j,k}(\tau(p)_{i,j,k})$ corresponds to the signal received by transducer k after the time $\tau(p)_{i,j,k}$ from transmission of transducer j in a sequential transmission i. The time $\tau(p)_{i,j,k}$ to time-of-fly from transducer k to point p and next to transducer j. The plane waves are transmitted at different angle for each sequential transmission i. The final image data synthetized via equation 5 is an input for attenuation estimator depicted above.

3. Measurements

Measurements were performed on a tissue mimicking phantom and on human liver *in-vivo*. The tissue mimicking phantom (1126 A, Dansk Phantom Service, Denmark) with uniform echogenicity and attenuation coefficient equal to 0.5 dB/cm/MHz. The phantom additionally contained a cylinder of 15 mm in diameter located at 30 mm depth. Regarding the echogenicity, the cylinder was identical to the surrounding medium. However, it had different attenuation coefficient value equal to 0.7 dB/cm/MHz. In order to compensate for diffraction effects a second phantom (1126 B, Dansk Phantom Service, Denmark) with uniform attenuation of 0.5 dB/cm/MHz was used as a reference.

The Verasonics Research System with attached linear probe L7-4 was used as a data acquisition device. The data from tissue mimicking phantom were acquired transmitting plane waves at the angles from range $[-25, 25]^\circ$ and the number of propagation angles was equal to 3. The data from human liver were acquired transmitting plane waves at the angles from range $[-15, 15]^\circ$ and the number of propagation angles was equal to 11. The pulse mean frequency was equal to $5MHz$ and the sampling frequency was equal to $20MHz$. The acquired RF lines were processed offline in Matlab. The processing consists of bandpass filtration and image data synthesis using SAFT technique. The mean frequency estimator window and the SSA window corresponds to $10mm$ and $8mm$ depth, for phantom and liver respectively. Similarly, the moving average filtration window corresponds to $10mm$ and $8mm$ lateral distance. The resulting standard B-mode and parametric images are presented in figures 1 and 2.

4. Results

The standard B-mode image and coresponding attenuation coefficient distribution of a attenuating cylinder in tissue phantom is presented at the figure 1. The cylinder is visible at the B-mode image, but it is vague and immersed in speckle noise. In fact, only upper and lower surfaces of the cylinder are visible. The attenuation of the cylinder differs only by $0.2dB/(MHz \cdot cm)$ from the background, thus the acoustic shadow, which could be mark the presence of a cylinder, practically does not exist. On the parametric attenuation image the cylinder is clearly visible. However, the size of the cylinder on the parametric image is smaller than in the reality. This is a result of loss of resolution due to using large windows in mean frequency estimator, the SSA algorithm and moving average filtration. The mean value of estimate from the area corresponding with location of the cylinder and the surroundings are equal $0.61 \pm 0.03dB/(MHz \cdot cm)$ and $0.5 \pm 0.1dB/(MHz \cdot cm)$ respectively. However, the value of the attenuation estimate corresponding with the center of the attenuating cylinder is equal

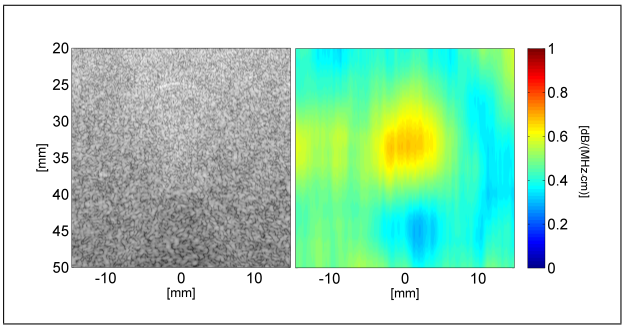

Figure 1. Standard B-mode image (left) and parametric attenuation image (right). The images present the tissue mimicking phantom with non-uniform attenuation.

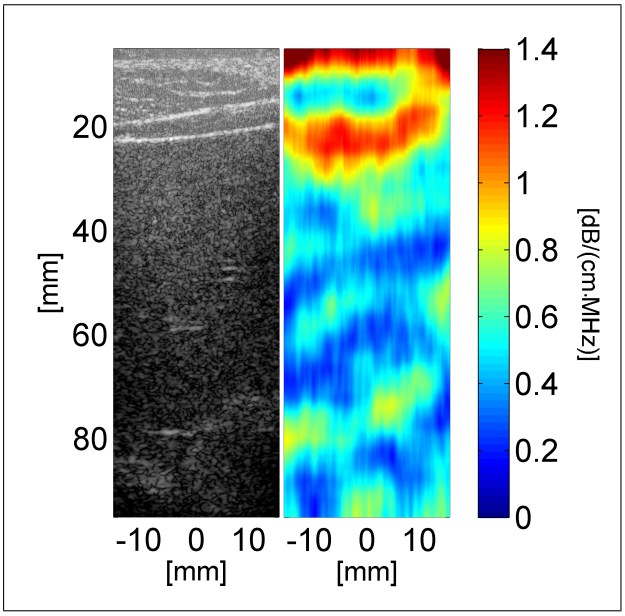

Figure 2. Standard B-mode image (left) and parametric attenuation image (right). The images present the fragment of human liver.

$0.7dB/MHz/cm$, thus it corresponds with the nominal attenuation of the cylinder. The underestimation of the mean attenuation of the cylinder is a next result of using large windows in processing algorithms.

The figure 2 presents the B-mode and parametric image of the human liver. The first layer in B-mode image (from 5 to $\sim 25mm$) presents the image of subcutaneous tissue, fat and muscle, while the deeper region presents the liver. At the parametric image the corresponding layers differs with attenuation and are clearly visible. However, the border between the upper layer and the liver is more fuzzy due to the size of the windows of processing algorithms. The mean value of attenuation estimate from depth between $5mm$ and $30mm$ is equal $0.9 \pm 0.3dB/MHz/cm$, while for deeper region, corresponding with the liver, the mean estimate is equal $0.5 \pm 0.1dB/MHz/cm$, which agree with the values presented in literature [18]. The higher mean attenuation of the upper layer could be explained by high muscle attenuation ($1.09dB/MHz/cm$ [18]).

5. Conclusions

The attenuation estimation method was presented. The method bases on tracking the mean frequency changes and assumes the propagation of a Gaussian pulse through linearly attenuating media. The input RF data were acquired using the SAFT scheme involving transmission of a quasi plane waves at different angles of incidence. Parametric images of tissue mimicking phantom and human liver were presented. In both cases estimated attenuation values are in expected range. The estimated attenuation for a tissue phantom agree with the geometry of a phantom and values declares by producer. However, the effect of large windows of processing algorithms (mean frequency estimator, SSA algorithm and moving average filtration) manifests itself by fuzzing the cylinder on the parametric image. The mean values of attenuation in human liver are in agreement with values presented in literature. The liver and the upper layer of a tissue can be distinguish on the parametric image. Thus, the presented attenuation estimation method can be used to produce attenuation parametric images of a soft tissue, however its relatively low resolution limits application. Nevertheless the parametric image gives different kind of information, comparing to B-mode and can assist the standard ultrasound images.

Acknowledgement

This work has been in part supported with project 2011/01/B/ST7/06728 financed by polish National Science Centre and project POIG.01.03.01-14-012/08-00 co-financed by the European Regional Development Fund under the Innovative Economy Operational Programme.

References

[1] Z. F. Lu, J. Zagzebski , F. T. Lee: Ultrasound Backscatter and Attenuation in Human Liver With Diffuse Disease. Ultrasound in Medicine & Biology, **25**, 7 (1999), 1047 1054.

[2] H. J. Nieminen, S. Saarakkala, M. S. Laasanen, J. Hirvonen, J. S. Jurvelin, J. Töyräs: Ultrasound Attenuation in Normal and Spontaneously Degenerated Articular Cartilage. Ultrasound in Medicine & Biology, **30**, 4 (2004), 493-500.

[3] V. Zderic, A. Keshavarzi , A. M. Andrew, S. Vaezy, R. W. Martin: Attenuation of Porcine Tissues In Vivo After High Intensity Ultrasound Treatment. Ultrasound in Medicine & Biology, **30**, 1 (2004), 61-66.

[4] A. E. Worthington, M. D. Sherar: Changes in UltrasoundProperties of Porcine Kidney Tissue During Heating. Ultrasound in Medicine & Biology, **27**, 5 (2001), 673-682.

[5] B. J. Oosterveld, J. M. Thijssen, P. C. Hartman, R. L. Romijn, G. J. Rosenbusch: Ultrasound attenuation and texture analysis of diffuse liver disease: methods and preliminary results. Physics in Medicine and Biology, **36**, 8 (1991), 1039-1064 .

[6] Y. Saijo, H. Sasaki: High Frequency Acoustic Properties of Tumor Tissue. - In: Ultrasonic Tissue Characterization. F. Dunn, M. Tanaka , S. Ohtsuki, Y. Saijo (eds.). Springer-Verlag Tokio, Hong-Kong, 1996.

[7] T. A. Bigelow, B. L. Mcfarlin, W. D. OŠbrien, Jr., M. L. Oelze: In vivo ultrasonic attenuation slope estimates for detection cervical ripening in rats: Preliminary results. Journal of Acoustical Society of America, **123**, 3 (2008), 1794-1800.

[8] B. L. Mcfarlin, T. A. Bigelow, Y. Laybed, W. D. O'brien, M. L. Oelze, J. S. Abramowicz: Ultrasonic attenuation estimation of the pregnant cervix: a preliminary results. Ultrasound in Obstetrics and Gynecology, **36** (2010), 218-225.

[9] T. A. Bigelow, Y. Laybed, B. L. Mcfarlin, W. D. O'brien, Jr: Comparison of algorithms for estimating ultrasound attenuation when predicting cervical remodeling in a rat model. Proc. 2011 IEEE International Symposium on Biomedical Imaging, 883-886.

[10] R. S. C. Cobbold: Foundations of Biomedical Ultrasound. Oxford University Press, 2007.

[11] P. Laugier, G. Berger, M. Fink, J. Perrin: Specular reflector noise: effect and correction for in vivo attenuation estimation. Ultrasound Imaging **7** (1985), 277-292.

[12] T. L. Szabo: Diagnostic Ultrasound Imaging: Inside Out. Elsevier Academic Press, 2004.

[13] D. H. Evans, W. N. McDicken: Doppler Ultrasound: Physics, Instrumentation and Signal Processing. John Wiley & Sons Ltd., 2000.

[14] Z. Klimonda, J. Litniewski, A. Nowicki: Spatial Resolution of Attenuation Imaging. Archives of Acoustics **34**, 4 (2009), 461-470.

[15] Z. Klimonda, J. Litniewski, A. Nowicki: Synthetic Aperture Technique Applied to Tissue Attenuation Imaging. Archives of Acoustics **36**, 4 (2011), 927-935.

[16] N. Golyandina, V. Nekrutkin, A. Ahigljavsky. Analysis of time Series Structure: SSA and related techniques. Chapman & Hall/CRC, 2001.

[17] G. Montaldo, M. Tanter, J. Bercoff, N. Benech, M. Fink: Coherent planewave compounding for very high frame rate ultrasonography and transient elastography. IEEE Transactions on Ultrasonics, Ferroelectrics and Frequency Control **56** (2009), 489-506.

[18] T. D. Mast: Empirical relationships between acoustic parameters in human soft tissues. Acoustics Res. Lett. **1** (2000), 37-42.